Environmental Technology & Innovation 27 (2022) 102498

Contents lists available at ScienceDirect

Environmental Technology & Innovation

journal homepage: www.elsevier.com/locate/eti

Decadal variations in CO_2 during agricultural seasons in India and role of management as sustainable approach

A. Singh [a,b], K. Abbhishek [a,c], J. Kuttippurath [a,*], S. Raj [a], N. Mallick [b], G. Chander [c], S. Dixit [c]

[a] CORAL, Indian Institute of Technology Kharagpur, Kharagpur 721302, India
[b] AGFE Department, Indian Institute of Technology Kharagpur, Kharagpur 721302, India
[c] International Crops Research Institute for the Semi-Arid Tropics (ICRISAT), Hyderabad, India

ARTICLE INFO

Article history:
Received 7 July 2021
Received in revised form 14 March 2022
Accepted 20 March 2022
Available online 25 March 2022

Keywords:
CO_2 trends
Climate change
Agriculture
Soil respiration
Agricultural management
Biochar

ABSTRACT

Atmospheric carbon dioxide (CO_2) is an important greenhouse gas (GHG) due to its high contribution to global warming. The CO_2 concentrations have increased significantly across the world after the industrialization. The anthropogenic provenance to the concentration of CO_2 needs immediate mitigative interventions. India is a global agricultural powerhouse and significantly contributing to the global CO_2 levels. Here, we present the changes in CO_2 concentrations between 2009 and 2020 in India with respect to agricultural activities. We also propose steps to reduce yield scaled soil emissions through agricultural management. The CO_2 concentrations in India show a steady increase of about 2.42 ppm/year from 2009 to 2020. The Central India (CEI), Hilly (HIL) and Indo-Gangetic Plain (IGP) show a relatively higher increase of about 2.43 ppm/year during the period. The highest CO_2 concentration is observed during *zaid* (March to May) season, whereas the lowest CO_2 concentration is observed during *kharif* (June to September) season. Anthropogenic activities such as the high use of fossil fuels and biomass burning are the two factors that significantly affect concentrations and temporal trends of CO_2 in India. A pilot-scale agricultural nutrient management experiment suggests that stable carbon alternatives like biochar can reduce soil CO_2 emissions without losing grain yield in paddy. Therefore, our analyses provide a better understanding of the spatio-temporal variations of CO_2 over India during agricultural seasons in relation to biomass burning, vegetation and anthropogenic activities. Furthermore, it suggests a policy implication for enforcing sustainable measures to reduce CO_2 emissions from agricultural activities in India.

1. Introduction

Atmospheric CO_2 is an important component of the global carbon cycle and also a major GHG. The global average concentration of atmospheric CO_2 has risen from 280 to 415 ppm (about 48%) post industrialization (Krishnapriya et al., 2020; Buchwitz et al., 2018). India contributes nearly 7% (as per an analysis performed 2018) to global GHG emissions (Olivier and Peters, 2019). The increase in atmospheric CO_2 can be attributed to anthropogenic activities such as the combustion of fossil fuels, forest degradation, edaphic factors and agriculture management practices. However, researchers

* Corresponding author.
E-mail address: jayan@coral.iitkgp.ac.in (J. Kuttippurath).

https://doi.org/10.1016/j.eti.2022.102498

are continuously trying and testing different alternatives to cut the carbon emissions of edaphic as well as anthropogenic origin.

Significant spatial and temporal variability in atmospheric CO_2 levels have been observed due to changes in the release and exchange of carbon in ecosystems. Activities altering the carbon balance also trigger global warming (Ekwurzel et al., 2017) and changes in the rainfall patterns (Kuttippurath et al., 2021), which have a snowballing impact on ecology, economy and global climate (IPCC, 2018; Kuttippurath and Raj, 2021). The balance between natural processes of carbon fixation and human activities, e.g., changes in agricultural land management practices, tillage and fertilization techniques, significantly alters the carbon balance and thus, needs immediate intervention. Consequently, processes of natural carbon balance in ecosystems have garnered public attention and studies have been done to identify primary atmospheric CO_2 sources and sinks in the troposphere. Based on previous studies, sources of CO_2 emissions can be broadly categorized into two types: natural and anthropogenic. Natural sources include soil organic carbon (SOC) decomposition, ocean release and basal respiration of organisms. Anthropogenic sources include industrial production, deforestation, burning of fossil fuels and modern agricultural practices (Leung et al., 2014).

However, it would be interesting to mention that atmospheric CO_2 is increasing at about half the rate of fossil fuel emissions, implying that the remaining CO_2 is either being fixed by terrestrial ecosystems or getting dissolved in the seawater (Heinze et al., 2015). Yet, the conditions worsen due to land-use changes (mainly deforestation) and conventional agricultural practices (i.e., fertilizer application). For instance, the application of chemical fertilizers leads to the release of more carbon from soils as CO_2, which has also made the agricultural systems an important anthropogenic source for atmospheric CO_2 (Chai et al., 2019). It has also been reported that conventional organic fertilizers like compost and farmyard manure increase the emission of CO_2 from soil under high soil moisture conditions (Brenzinger et al., 2018). Nevertheless, Case et al. (2014) has indicated that stable carbon alternatives like biochar can reduce the soil CO_2 emissions, but its feasibility under high soil moisture conditions needs close monitoring and thus demands further investigation.

Satellite observation is a reliable technique to monitor the changes of trace gases in the atmosphere. However, the studies carried out over India in the last two decades demand keen analyses to understand the role of anthropogenic sources and natural sinks of CO_2 over India (Nayak et al., 2011; Preethi et al., 2011; Tiwari et al., 2011, 2013; Nalini et al., 2018; Gupta et al., 2019). Ground-based observations of CO_2 are of much importance in understanding the role of anthropogenic sources like agricultural activities. Although, a few ground-based observations of atmospheric CO_2 are reported over the Himalaya and western India, but their observation period is very short (Anthwal et al., 2009; Sharma et al., 2014; Mahesh et al., 2016). Traditionally, ambient CO_2 concentration monitoring is usually based on observations from ground stations spanning around the world. For instance, the global average monthly CO_2 concentration above 400 ppm was measured in 2015 (March–May) at Mauna Loa (direct atmospheric CO_2 measuring station), which also holds the longest CO_2 measurement record available (Dlugokencky and Tans, 2015). These atmospheric measurements are accurate and thus capture even a small variation in atmospheric CO_2 concentrations (Le Quere et al., 2009). However, such field measurements are limited (Gurney et al., 2002; Boesch et al., 2011) and therefore, the alternative way is to use satellite measurements.

Prasad et al. (2014) presented the annual and seasonal variation in CO_2 concentration over India using GOSAT (Greenhouse Gases Observing Satellite) data for two years (2009–2011) and compared it with SCIAMACHY (Scanning Imaging Absorption Spectrometer for Atmospheric Chartography) CO_2 data. Similarly, Gupta et al. (2019) presented the seasonal and interannual variability of CO_2 over India using nine years of AIRS data from 2003 to 2011. They reported that the CO_2 over India has been increasing at the rate of 2.01 ppm/year from 2003 to 2011. Therefore, we have studies which indicate the shaping of spatial and temporal variability in CO_2 concentration over India. However, there is a dearth of studies explaining the variability originating from anthropogenic activities during agricultural seasons.

The role of soil respiration in the increase of CO_2 concentration over India is important as most of the land use in India is related to agricultural activities. We designed this study to observe the spatial and temporal variability in CO_2 concentration over India during the agricultural seasons. Here, we present the CO_2 variation during the agriculture management intensive and management non-intensive periods and the role of different fertilization techniques on soil respiration in high moisture conditions. In addition, we also present the recent trends in CO_2 over India using GOSAT data from 2009 to 2020. Our results from a pilot experiment aimed at testing possible interventions in soil fertilization strategies to cut the emissions originating from soil respiration. We have used paddy as a test crop in this experimental study as it is an important cereal crop in India and staple food crop in Asia. The global rice production share of Asia is about 90.6% for 1994–2019 (FAOSTAT, 2019). The rice predominantly releases methane (Singh et al., 2021), but the direct seeding rice (DSR) cultivation and upland rice also contribute to atmospheric CO_2 emissions (Neue, 1993). The DSR cultivation techniques are gaining popularity in India as they require fewer resources than conventional practices (Kaur and Singh, 2017). However, India, in its INDC (Intended Nationally Determined Contributions) to the UN Framework Convention on Climate Change (UNFCCC) has pledged to cut the emission intensity of its GDP (Gross domestic product) by 33 to 35% over 2005 levels by 2030 (Dubash et al., 2018; Lakshmanan et al., 2017). The growing resource-demand escalated the anthropogenic emissions of CO_2 by fossil fuel combustion, deforestation, cement manufacture and contemporary farming techniques. This study explores the enhancement of atmospheric CO_2 over India owing to biospheric fluxes like heterotrophic respiration and soil emissions. The long range transport through winds along with local CO_2 emission sources play a major role in deciding the spatio-temporal changes. However, such sources located over vast stretch of croplands in India can be regulated through policy interventions in agricultural activities, such that the increasing rate of atmospheric CO_2 can be placed under control by cutting emissions at the source. Therefore, our study provides valuable insights that would help in making policy level decisions.

2. Material and methods

Carbon dioxide data

The CO_2 data from GOSAT is used, which is a sun-synchronous polar orbit satellite placed at an altitude of about 666 km in January 2009. It is dedicated to measure atmospheric CO_2 and methane (CH_4) in the atmosphere of Earth using TANSO-FTS (Thermal and Near Infrared Sensor for Carbon Observation-Fourier Transform Spectrometer) (Kuze et al., 2009). It was developed under joint collaboration of Japan Aerospace Exploration Agency (JAXA), Ministry of Environment (MOE) and National Institute for Environmental Studies (NIES) of Japan. The overpass time of GOSAT is 13:00 (local time) every three days, and the diameter of the footprint in nadir is approximately 10 km. The TANSO-FTS detects reflected sunlight in CO_2 and CH_4 absorption bands in shortwave infrared (SWIR) wavelengths between 0.758 and 2.08 μm. It has a spectral resolution of 0.2 cm^{-1} and can retrieve ozone, water vapour and mid-tropospheric CO_2 by measuring thermal emission between 5.56 and 14.3 μm. Another sensor in GOSAT is TANSO-CAI (Cloud and Aerosol Imager), which is used to screen cloudy pixels during the retrieval process (Morino et al., 2011). In general, the measurement of CO_2 by GOSAT is in accordance with other approaches of GHG monitoring that include ground-based, balloons, ships, tall towers and balloon measurements (Inoue et al., 2013; Zhang et al., 2014). Here, we have used NIES full physics SWIR L3 (Level 3) version 02.81 dataset of GOSAT CO_2 over India from 2009 to 2020. The SWIR L3 products are the estimated results of column-averaged concentrations for one month on a global 2.5° by 2.5° grid, based on the column abundances of carbon dioxide (XCO2) of the SWIR L2 products by the spatial statistical method, i.e., Kriging (Watanabe et al., 2015). The retrieved CO_2 data have been validated using CO_2 observation at selected TCCON (Total Column Carbon Observation Network) measurements and showed a bias and standard deviation of about −0.33 ppm and 2.17 ppm, respectively, for XCO2 (Morino et al., 2019).

Ancillary data

Normalized Difference Vegetation Index (NDVI) and Net primary productivity (NPP)

Normalized Difference Vegetation Index (NDVI) is the most widely used vegetation index and broadly indicates plant photosynthetic activity and aboveground primary production (Chhabra and Gohel, 2019). It quantifies vegetation by measuring the difference between near-infrared (which vegetation strongly reflects) and red light (which vegetation absorbs). Its value varies from 0 (minimum) to 1 (maximum). Vigorous vegetation growth is denoted by the maximum value of NDVI (Chhabra and Gohel, 2019). Changes in the vegetation activity are driven by multiple natural and anthropogenic factors that can be reflected in satellite derived NDVI products. NPP is the net carbon gain by plants, which is the balance between carbon gained by gross primary production (GPP – i.e., net photosynthesis measured at the ecosystem scale) and carbon released by plant mitochondrial respiration, both expressed per unit land area. It includes the new biomass produced by plants, the soluble organic compounds that diffuse or are secreted into the environment (root or phytoplankton exudation), the carbon transfers to microbes that are symbiotically associated with roots (e.g., mycorrhizae and nitrogen-fixing bacteria), and the volatile emissions that are lost from leaves to the atmosphere (Clark et al., 2001). We have used Moderate Resolution Imaging Spectroradiometer (MODIS)-derived NDVI and NPP data. The MOD13C2 Version 6 for NDVI and MOD17A3 for NPP. These are cloud-free spatial composites of the gridded 16-day 1-kilometre data and are provided as a level-3 (L3) product projected on a 0.05° (5600-metre) geographic Climate Modelling Grid (CMG).

Open-Source Data Inventory for Anthropogenic CO_2(ODIAC)

Open-Source Data Inventory for Anthropogenic CO_2 (ODIAC) effectively quantifies CO_2 emissions from the anthropogenic activities during a month in the atmosphere (unit: g $CO_2/m^2/d$). It includes emissions from cement manufacturing, thermal power generation and fossil fuels (Oda and Maksyutov, 2011).

Global Fire Emissions Database (GFEDv4.1s) and other datasets

Global Fire Emissions Database (GFEDv4.1s) quantifies aerosol and trace gas emissions due to biomass burning (BB). CO_2 emissions during the BB (unit: g CO_2/m^2/month) activities are estimated by using biogeochemical model-simulated fuel loads, land-cover based emission factors, moisture-regulated combustion factors and satellite-retrieved burned area data (Van Der Werf et al., 2017). We calculated the monthly fire CO_2 emissions from various types of biomasses burning from 2009 to 2020. The agriculture land use (ALU) CO_2 emissions, Net stock change (C) over cropland organic soils and mineral fertilizer data between 2009 and 2020 are obtained from FAOSTAT (Food and Agriculture Organization Corporate Statistical Database). The electricity consumption for agriculture purposes, the total number of power tillers and tractors sold data are taken from the State of Indian Agriculture 2017–18 report. The total cropped area and share of the total power data are obtained from the IndiaAgristat data portal. The net ecosystem exchange (NEE) is a measure of the net exchange of C (Carbon) between an ecosystem and atmosphere (per unit ground area), and is the primary gauge of ecosystem C sink strength (Kramer et al., 2002). A Data-driven Upscale Product of NEE version 2020.2 is used in this study. The spatial and temporal resolutions of the data are 0.1° × 0.1° and 10 days, respectively (Zeng et al., 2020).

The HYSPLIT trajectory model

The Hybrid Single-Particle Lagrangian Integrated Trajectory (HySPLIT) model was employed to estimate air mass transport to determine their origin and source–receptor relationships (Stein et al., 2015). We computed a 7-day back-trajectory starting six different points in all six regions (NEI, IGP, HIL, NWI, PI and CEN)/agrarian zones of India

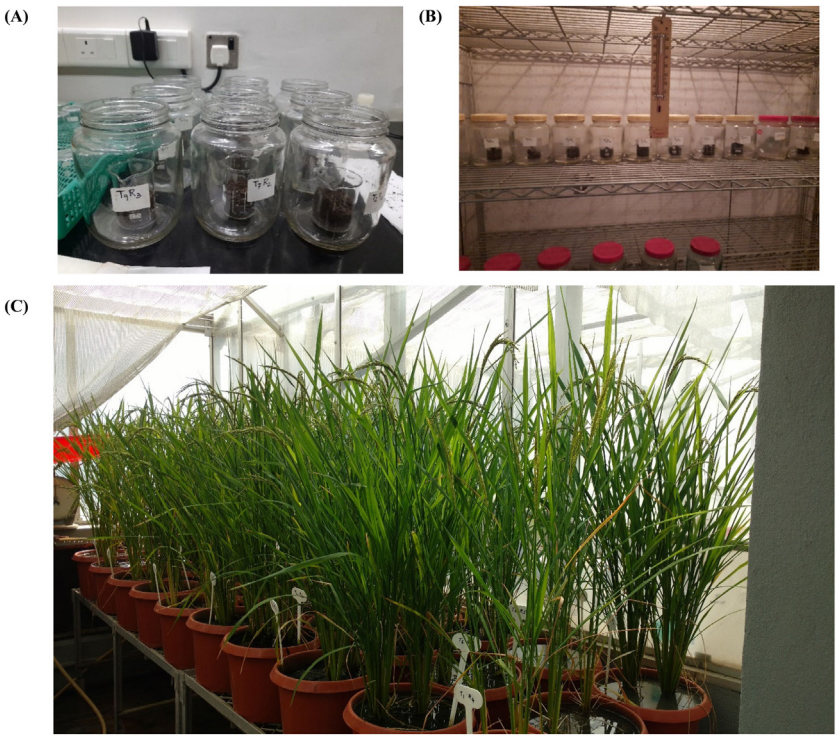

Fig. 1. The experimental setup showing loading of soil samples in respiration jars (A), incubation chamber at 25 °C temperature with sealed soil respiration setup (B) and glass house setup with paddy crop(C).

identified to find source and receptor. Horizontal and vertical wind components, geopotential height, temperature, and relative humidity in 3-dimension, and pressure, temperature, precipitation, horizontal momentum flux, horizontal wind components, sensible and latent heat fluxes, radiation fluxes at the surface are considered for the back trajectory calculations (Jin et al., 2021). Trajectories are grouped through multivariate cluster analysis using the angle distance (Sirois and Bottenheim, 1995), defined using the law of cosines to identify the main flow and source region, and quantify its contribution. The air mass transport is calculated using different vertical level data from the Global Data Assimilation System (GODAS; Behringer and Xue, 2004).

Experimental design and setup

We tested the effect of different fertilizer application strategies involving sole and integrated applications of biochar vis-à-vis compost on basal soil respiration through a two-year controlled environment greenhouse study conducted in a completely randomized experimental design. The nutrient management treatments comprised different doses of biochar and compost with and without mineral fertilizers as different nutrient management strategies in paddy cultivation (see Table 1). The treatments are replicated six times and the results are analysed using one way ANOVA. The experimental soil belongs to Vertisol order of U.S. soil Taxonomy and is filled in 1300 cm^3 pots, which were planted with two rice plants per pot (Fig. 1). The required crop management is done during rice plant crop growth phase following the methods by Nayak et al. (2019). The nutrients N (nitrogen), P (phosphorus) and K (potassium) are supplied in the form of Urea, single superphosphate (SSP) and muriate of potash (MOP), respectively. The mineral fertilizers are applied as concentrated solution evenly in pots, the day before planting, while biofertilizers (organic fertilizers) are mixed thoroughly in the topsoil (5 cm). All the mineral fertilizers are applied basal as of their full dose except mineral N, which is applied 50% basal and 50% at the panicle development stage. The soil from each pot at different growth stages of paddy (i.e., Active tillering (AT), Panicle initiation (PI), and maturity (Harvesting stage) is collected using a core sampler and analysed for the CO_2 emission originating from the heterotrophic soil respiration for different fertilizer regimes in paddy. After the estimation of emissions, the soil was returned to its original position in the respective pots. We used the basal trap method using NaOH (2.0 M) in air-tight sealed soil respiration jars with NaOH blanks (control) and treatment samples to calculate CO_2 flux as explained in Haney et al. (2002). The setup is incubated at 25° C for 24 h to capture the CO_2 produced using NaOH and $BaCl_2$, which was back-titrated with 1 M HCl with phenolphthalein as an indicator to determine the amount of CO_2 evolved using equation (Schinner et al., 1995):

$$Treatment\ carbon\ dioxide\ emission = \frac{(V - S) \times 2.2 \times 10^2}{Soil\ weight(\%dm)}$$

Table 1
Details of Experimental treatments formulated based on different fertilizer components and soil amendments. The details of grain yield are expressed as mean ± sd.

T. No.	Nutrient management treatments	Nutrient management treatments abbreviation	Urea (g)	Single super phosphate (g)	Muriate of potash (g)	Zinc sulphate (g)	Compost (g)	Biochar (g)	Grain yield (g/hill)
T1	Control without any fertilizer application	Con	–	–	–	–	–	–	4.61 ± 0.4^{a}
T2	NPK[¥] at recommended dose (farmer's practice)	CF-REC	1.50	2.00	0.65	–	–	–	23.581 ± 1.2^{d}
T3	Soil-test based NPK + deficient micronutrients (STB)	CF-STB	1.72	2.50	0.50	0.47	–	–	30.191 ± 1.0^{f}
T4	Sole biochar application (@100% N equivalence)	BC100	–	–	–	–	–	76.36	17.801 ± 0.3^{b}
T5	Sole compost application (@100% N equivalence)	CO100	–	–	–	–	76.36	–	21.691 ± 1.4^{c}
T6	Low-dose biochar based INM[¶] (75% STB + Biochar @25% N equivalence)	CF75 + BC25	1.29	1.87	0.37	0.35	–	19.00	37.651 ± 0.3^{g}
T7	Low-dose compost based INM (75% STB + Compost @25% N equivalence)	CF75 + CO25	1.29	1.87	0.37	0.35	19.00	–	27.961 ± 0.5^{e}
T8	High-dose biochar based INM (50% STB + Biochar @50% N equivalence)	CF50 + BC50	0.86	1.25	0.25	0.23	–	38.18	28.281 ± 1.6^{e}
T9	High-dose compost based INM (50% STB + Compost @50% N equivalence)	CF50 + CO50	0.86	1.25	0.25	0.23	38.18	–	23.351 ± 1.0^{cd}

Note: NPK[¥] means Nitrogen (N), Phosphorus (P2O5), and Potassium (K2O); INM[¶] means Integrated nutrient management; Different alphabets in particular column superscripts represent significant difference amongst treatment.

Where V is the mean volume of HCl consumed by controls, S is the mean volume of HCl consumed by samples, dm is dry matter, and 2.2 is the conversion factor for 0.1 M HCl to CO_2.

3. Results and discussion

3.1. Seasonal variability in atmospheric CO_2

Fig. 2 shows the monthly variation of atmospheric CO_2 concentrations averaged for the study period (i.e., 2009–2020) over India. Although the seasonality in atmospheric CO_2 is mainly influenced by the transport processes (viz. Convection, Advection and Diffusion), as explained in Krishnapriya et al. (2020), the variations near-surface have strong source correlations (Shusterman et al., 2018). Since India has diverse topographical features, the vegetation scenarios also differ from one region to the other. Therefore, to study the seasonal changes in CO_2 concentration, we have conceptually divided India into six different regions, as shown in Figure S1. We analyse the variation in CO_2 concentration during the three agricultural seasons, namely *kharif* (June to September), *rabi* (October to February) and *zaid* (March to May) from 2009 to 2020 over India (Fig. 2) and compare it with NDVI and NEE. The NDVI represents aboveground primary production and thus, effectively detects the changes in productivity of the terrestrial ecosystem (Chhabra and Gohel, 2019). The NEE is a measure of the net exchange of C between an ecosystem and the atmosphere (per unit ground area) and is a primary gauge of ecosystem C sink strength (Kramer et al., 2002). Our analyses reveal that the CO_2 concentration is lowest in India during the agricultural *kharif* season. It increases in *rabi* and reaches the maximum value in the *zaid* season in India.

In general, CO_2 concentration shows a gradual increase from January to May. A concentration of about 398 ppm is observed in January, which increases to 400 ppm by March and the peak concentration of about 402 ppm is found in May. The highest concentration in May can be partly explained on the basis of convection and planetary boundary layer height (Gupta et al., 2019). However, the concentration decreases in June and July due to the horizontal transport of CO_2 depleted air parcels from the oceanic regions to India by southwest monsoon winds, and it again increases slightly in August (Fig. 2). For instance, to examine the air mass transport to the Indian land regions, we selected 6 points in 6 regions and computed the back-trajectories for the agricultural seasons. It shows that the air mass is coming from the oceanic region in Kharif season, about 50–80% in all regions, except in HIL where the air mass is transported from the northern land regions. However, as vegetation plays a significant role in fixing atmospheric CO_2 during agricultural seasons (Chhabra and Gohel, 2019), an offset from the edaphic release of carbon through soil respiration and oxidation of soil organic matter (SOM) decreases the impact. This has been discussed in Krishnapriya et al. (2020) using model results, where the vertical diffusion causes negative input to net CO_2 budget. India receives monsoon rainfall in *kharif* season, which significantly affects the atmospheric CO_2 concentrations and subsequently, the crop response alters the carbon budget of the ecosystem. As per an estimate, the southwest monsoon brings in about 90% of rainfall in India during the *kharif* season, when intensive agricultural activities occur throughout the country. The CO_2 concentration starts decreasing during this period and therefore, the lowest concentration is observed in the *kharif* (June to September) season. This seasonal reduction in CO_2 might also get affected from the meso-convective process, deposition of HCO_3 (Iavorivska et al., 2016), along with enhanced photosynthetic fixation due to the increased soil moisture and vegetation cover (Chhabra and Gohel, 2019; Gupta et al., 2019). Since there is high CO_2 uptake by vegetation, we observe negative or nearly zero NEE in most regions in this season. Furthermore, the presence of clouds during this season decreases the air temperature, thereby reducing the leaf and soil respiration rate, which eventually increases the carbon uptake (Sreenivas et al., 2016).

Furthermore, our analyses show that CO_2 concentration reaches a minimum of 392 ppm in September and a gradual increase from October to December in India. The reason for such large variability in atmospheric CO_2 concentration is the seasonal activities that alter the atmospheric carbon balance. For instance, the mainland of India experiences the northeast monsoon winds in horizontal and vertical directions, causing upwelling of CO_2 enriched air in this season; resulting in net gain in the surface CO_2 concentrations (Krishnapriya et al., 2020). This might be a reason for the gradual increase in the CO_2 concentration in the rabi (October to February) season. The seasonal increase in CO_2 concentration with the onset of the agricultural season might also find a relation with the land preparation activities before crops are sown, which releases CO_2 trapped in soil layers. However, due to this transition, the net photosynthesis from vegetation over croplands is significantly reduced during the initial period of *rabi* season (Chhabra and Gohel, 2019). The *rabi* crops are also called winter crops as they are cultivated between October and February, resulting in differential growth rates during winter months (December to February). Therefore, strong respiration and weak photosynthesis take place during the early crop growth stage, which contribute significantly to enhanced levels of CO_2 concentration in the atmosphere. Apart from these, the air mass is transported from the northwest land regions in this season at all regions, about 85%. However, the peninsular India receive much of its air mass (95%) from the Bay of Bengal in this season, which makes the relatively lower CO_2 concentrations there.

Anthropogenic activities like irrigation through diesel pumps during the winter months consume large amounts of fossil fuel energy, ensuring the release of CO_2 into the atmosphere. In addition, there is no or little precipitation over most regions of India during this period and *rabi* crops are cultivated depending on residual soil moisture. Therefore, vegetation in this season is greatly reduced in most areas of India as observed with lower NDVI values during *rabi* season compared to that in the *kharif* season, except for places like the Peninsular India (PI) region. As a result, CO_2 uptake by

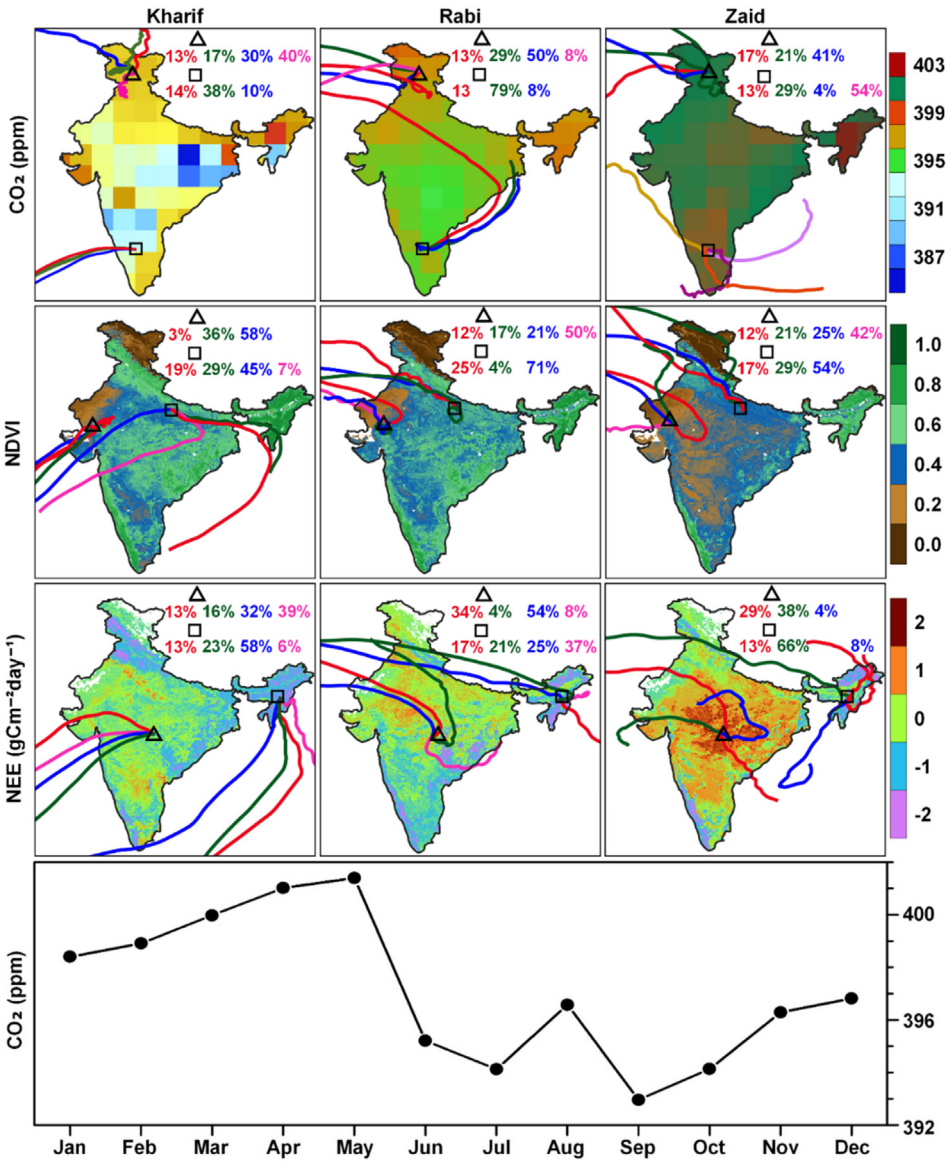

Fig. 2. Seasonal distribution of atmospheric carbon dioxide concentration, NDVI and NEE averaged for the period 2009–2020 over Indian region: *Kharif* (June to September), *Rabi* (October to February) and *Zaid* (March to May). Monthly variation of CO_2 over India averaged between 2009 and 2020. The 7-day back trajectories at different points in different regions of India at a surface level during Kharif (June to September), Rabi (October to February) and Zaid (March to May) are also shown. Only two trajectory points are shown in each illustration for clarity reasons.

plants is also reduced and thus, we observe higher NEE in the *rabi* season as compared to that in *kharif*. The eastern coast regions receive rainfall during the northeast monsoon, resulting in major agricultural activities during these months. Rain helps to wash out most of the atmospheric CO_2, causing the lowest CO_2 concentration in the PI region during this season, in addition to the low CO_2 air transported from the Bay of Bengal during the season, as discussed before. Besides, during the onset of *kharif* (June/July) and towards the end of *rabi* (January), the association of CO_2 and NDVI is reversed as an increase in one might offset the other (Gupta et al., 2019).

The highest CO_2 concentration in the agricultural *zaid* season might be because of fallow croplands due to the unavailability of farm irrigation facilities. This decreases vegetation cover, as reflected by the lower NDVI values in this season. However, an increase in the land surface temperature might lead to loss of soil moisture, causing the release of trapped CO_2 in soils due to accelerated decomposition of SOM. In addition, our trajectory analysis show that the air parcels carrying atmospheric CO_2 mostly traverses large land area (Fig. 2) before reaching to each region as described in this study (Figure S1). The atmospheric circulation therefore builds a strong concentration of CO_2 over the identified regions in India. For instance, the air mass is travelled through the land regions, about 70–80% of air mass there. Nevertheless,

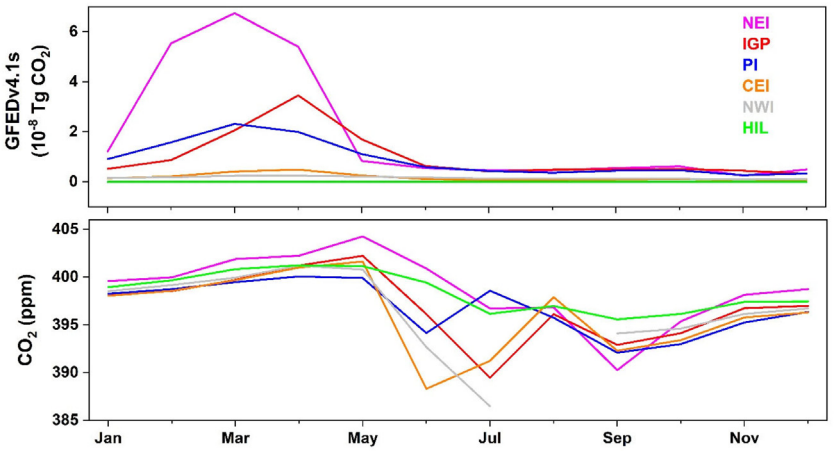

Fig. 3. The monthly distribution of biomass burning emission (GFEDv4.1s) inventory and CO_2 concentration at different regions of India [Indo-Gangetic Plains (IGP), Peninsular India (PI), North-West (NWI), Central India (CEI), North-East India (NEI) and Hilly (HIL), as illustrated in Figure S1]. The data are averaged from 2009 to 2020.

the PI and NEI receives air masses also from the oceanic regions and is the reason for the relatively lower CO_2 in those regions. Although, vegetation acts as a carbon sink, its strength decreases with a reduction in cropping during the *zaid* season, which further promotes such high concentration. Henceforth, positive NEE is observed due to decrease in the CO_2 uptake by vegetation and this indicates that the ecosystem was a source of CO_2 during this season. Our inferences find support from earlier findings indicating that high daytime temperature during April–May (dry season) creates a tendency for the ecosystem to become a moderate source of carbon exchange (Patra et al., 2013). Nevertheless, despite moderate temperature and the largest forest cover, NEI shows the highest CO_2 concentration of 402 ppm compared to other regions of India. This might be due to incidences of forest fires during the dry season in NEI (Kuttippurath et al., 2020). Furthermore, the low wind speed during the *zaid* season (MAM) causes weak mixing in the atmospheric boundary layer, contributing to a higher CO_2 concentration over India (Sharma et al., 2012). In contrast, PI shows the lowest CO_2 concentration of 399 ppm in the *zaid* season.

The spatial distribution of atmospheric CO_2 concentration over India, nevertheless, shows a consistent pattern in all seasons. In India, the HIL and NEI regions have the highest concentration of atmospheric CO_2 in all seasons. In contrast, the lowest CO_2 concentration is present over PI in all four seasons. The shifting cultivation is still practised in the North-East India and thus, higher CO_2 concentration is observed in those regions (Pasha et al., 2020). Shifting cultivation involves clearing the primary or secondary forest through the slash and burn process and the crop cultivation thereafter, for 1–3 years, followed by a fallow phase, during which cultivation is suspended to allow recovery of soil fertility (Bhuyan, 2019). Biomass burning results in increased atmospheric CO_2 emissions (Yang and Zhao, 2018; Shi et al., 2017). Here, we have used biomass burning emission inventory (GFEDv4.1s) to identify the major biomass burning activities occurring in different regions of India (Fig. 3). Significant fire events can be observed in NEI, IGP and PI regions from February to May. Additionally, the highest CO_2 emissions from biomass burning are observed during *zaid*, contributing to the highest concentration of CO_2 during that season (March to May). However, it can be noted that IGP shows a double peak in CO_2 emissions occurring from crop residue burning in its annual cropping cycle corresponding to the two major harvest seasons, i.e., *kharif* and *rabi* (Kuttippurath et al., 2020; Venkataraman et al., 2006). Similarly, the peaks appearing in February–March in the PI region are consistent with the major harvest season there. The largest amount of CO_2 emission from biomass burning over NEI in March might be due to the practice of shifting cultivation (i.e., a particular method of farming). Therefore, agricultural activities play a crucial role in determining the spatial and temporal variations of CO_2 concentration over India, which is also influenced by the lighter and finer operations carried out in the soil, between sowing and harvesting (intercultural operations/activities) during the growing season.

3.2. Agro management mediated variations in carbon dioxide

We have used NDVI, NPP and NEE as proxy to examine spatial and temporal changes in the terrestrial ecosystem productivity directly influenced by atmospheric CO_2 (Clark et al., 2001; Kramer et al., 2002). The agricultural activities in India are releasing a large amount of carbon into the atmosphere, which influences these proxies over time. Therefore, to determine the role of intercultural activities on atmospheric CO_2 and to visualize associated changes in NDVI and NPP, we present this agro-management (semi-annual) analysis of CO_2 concentration over India for the period 2009–2020 (Fig. 4). We divide the whole year into two periods based on the agricultural management practices: management intensive period (July–December) and management non-intensive period (January–June). The seasonal changes in NEE were strongly

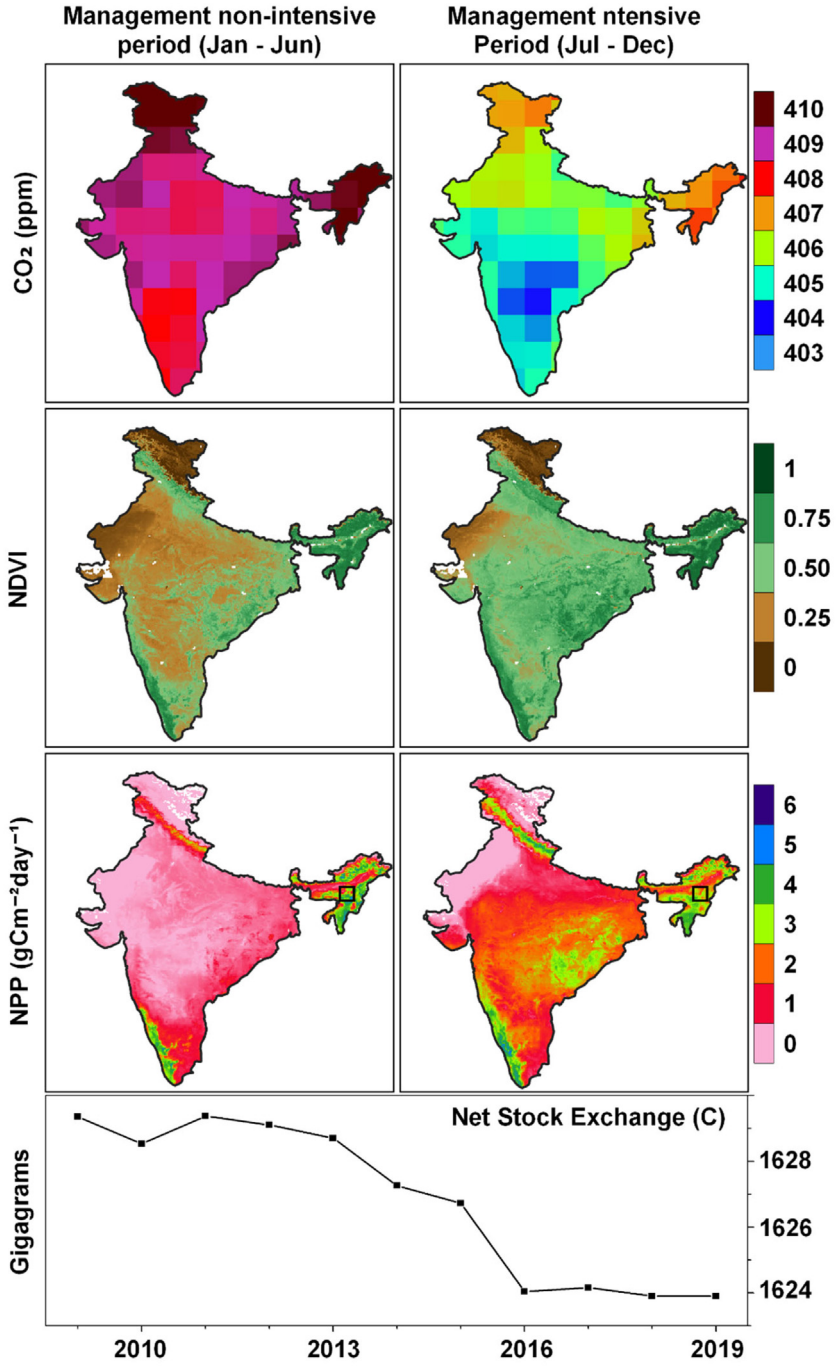

Fig. 4. Agro management (semi-annual) distribution of atmospheric carbon dioxide, NDVI (Normalized Difference Vegetation Index) and NPP (Net Primary Productivity, 2009–2016) in India from 2009 to 2020. Net stock change (C) over cropland organic soils from 2009 to 2019 in India.

regulated by soil moisture. Therefore, we present the NEE with the soil moisture and land surface temperature (Figure S2) for management intensive period and management non-intensive period in India. The period from January to June generally does not experience any opening of soil at mass scale through tillage except summer ploughing at some places. However, the period from July to December witnesses the opening up of soil several times during sowing and intercultural operations for the major agricultural seasons of *rabi* and *kharif*. Apart from this, the soil moisture is quite high during the management intensive period, and the land surface temperature is low (Singh et al., 2021). These conditions provide the opportunity for methanogenesis rather than the oxidation of soil organic carbon (SOC) stock. However, our analysis shows

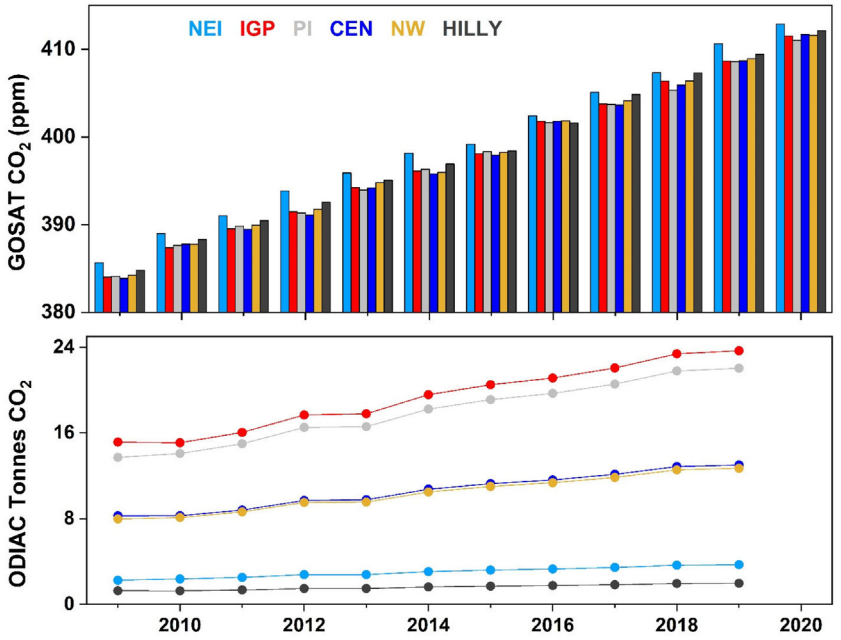

Fig. 5. The Inter-annual variations of GOSAT carbon dioxide and ODIAC CO_2 emissions at different regions of India [Indo-Gangetic Plains (IGP), Peninsular India (PI), North-West (NWI), Central India (CEI), North-East India (NEI) and Hilly (HIL), as illustrated in Figure S1] from 2009 to 2020.

that even organically managed soils are showing an overall decrease in the net stock of carbon (Fig. 4) between 2009 and 2019, which suggests the loss of SOC in the last decade.

The management non-intensive period shows a higher concentration of CO_2 than the management intensive period, which might be attributed to the higher land surface temperature and low soil moisture promoting the oxidation of SOC. This is interesting as it also highlights the role of crop cover over arable lands that fixes atmospheric CO_2. During this period, most agricultural lands remain fallow due to the unavailability of water for irrigation, so the vegetation cover is reduced to a greater extent and hence, the CO_2 uptake is also decreased. Therefore, positive NEE is observed and this indicates that the ecosystem was a source of CO_2 in this dry period between January and June (Table S1). However, it has also been found that the agricultural land gets exposed to soil erosion due to the unavailability of vegetation cover. The accelerated soil erosion has been identified as a source of GHG emissions (Lal, 2019) to the atmosphere. Lal and Pimentel (2008) have reported that soil erosion has a negative impact on carbon sequestration, constituting a source of atmospheric CO_2. Furthermore, they state that soil erosion increases CO_2 emissions due to decrease in NPP on eroded soil and a relatively high decomposition of SOC in buried sediments. In the early months of the non-intensive period (January–February), the lower temperature inhibits the microorganism activity that hinders the decomposition process. However, the temperature starts increasing in the latter half of this period (March to May), which enhances the microorganism activity promoting the decomposition and CO_2 release, as shown by the high CO_2 concentration during the *zaid* season in our analyses (Fig. 2). Conversely, during the management intensive period, most agricultural land undergoes cultivation. Temperature, precipitation, soil moisture and light hours are optimum for attaining the required thermal units for vegetation growth and this enhances the photosynthesis in this period. During photosynthesis, plants uptake a considerable amount of CO_2 from the atmosphere (Daniel, 2010). Thus, high CO_2 uptake by vegetation during management intensive period. We observe negative or nearly zero NEE in most of the Indian regions and shows higher values of NDVI and NPP due to the extensive vegetation cover over the arable lands in this period. Therefore, terrestrial vegetation is a strong driver in controlling the CO_2 concentration in the atmosphere than intercultural activities.

3.3. Inter-annual variations in atmospheric carbon dioxide

Our analyses show a significant increase in CO_2 from 384 ppm in 2009 to 411 ppm in 2020 (Fig. 5) over India. Emissions from human activities are one of the major contributors to this increase in CO_2 levels in the atmosphere (Oda and Maksyutov, 2011). Therefore, to quantify the CO_2 emissions due to anthropogenic activities, we have analysed the ODIAC (Open-Data Inventory for Anthropogenic Carbon dioxide) CO_2 data over India from 2009 to 2019 (Fig. 5). Note that this inventory is based only on the anthropogenic CO_2. The ODIAC CO_2 emissions show a consistent increase between 2009 and 2019 throughout India; confirming that anthropogenic activities are one of the key drivers of the increase in atmospheric CO_2 from 2009 to 2020 in India. Additionally, the land-use changes may directly influence the global carbon

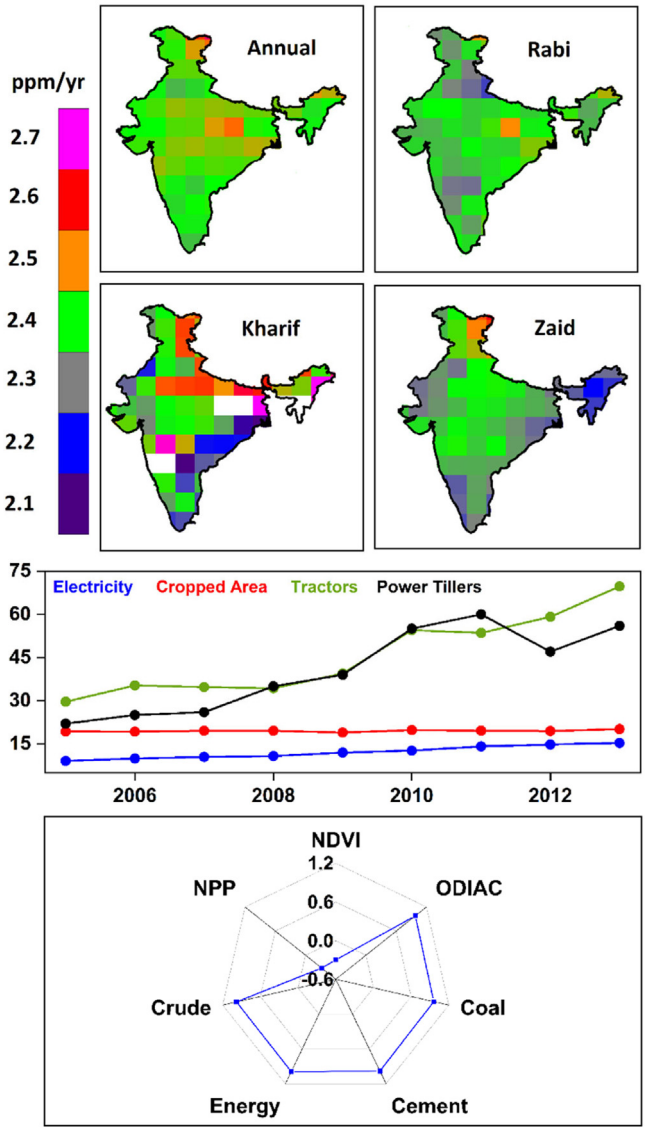

Fig. 6. The GOSAT CO_2 trends estimated from measurements of seasonal and annual average over India from 2009 to 2020 (yr = year). All the trends are statistically significant at 95% CI. Inter-annual distribution of Electricity Consumption for Agriculture purposes (10^4 GWH), Total Cropped Area (10^7 ha), Tractors Sold (10^4 numbers) and Power Tillers sold (10^3 numbers) from 2005 to 2013 in India. The correlation coefficient between atmospheric CO_2 and its drivers over India.

budget and trends in atmospheric CO_2. After the industrialization in 1850, enhanced anthropogenic activities and changes in land-use patterns led to the degradation of soil and huge emission of CO_2 into the atmosphere (Smith et al., 2007). The CO_2 emissions from agriculture land use (ALU) in India increased from 2009 to 2017 (Figure S3). Furthermore, the trend analysis for the annual CO_2 concentration shows a significant increase of about 2.42 ppm/year between 2009 and 2020 (Fig. 6). The CEI, IGP, HIL and North-West (NWI) regions show a significant increase of about 2.44, 2.43, 2.43 and 2.41 ppm/year, respectively, in their annual CO_2 concentrations between 2009 and 2020.

The consumption of petroleum products increased by about 4.7% CAGR (Compound annual growth rate) in India between 2010 and 2019 (Source: Indian petroleum & natural gas statistics 2019–20), which correlates with the rise in demand for tractors and power tillers for agricultural activities. The share of tractors in the total farm power has increased substantially as the sale of tractors and power tillers has increased about 6% (CAGR) over the period 2005–2017 (Source: State of Indian Agriculture 2017–18). There is a significant increase in CO_2 emissions from different sectors of India in 2009–2018, as observed in EDGAR analyses (Table S2). Approximately 65% increase in CO_2 emissions from the transport sector in India between 2009 and 2018. Additionally, India ranks second in the world for coal consumption. There is a continuous increase in coal consumption between 2008 and 2017, and can be attributed to the increased dependence of

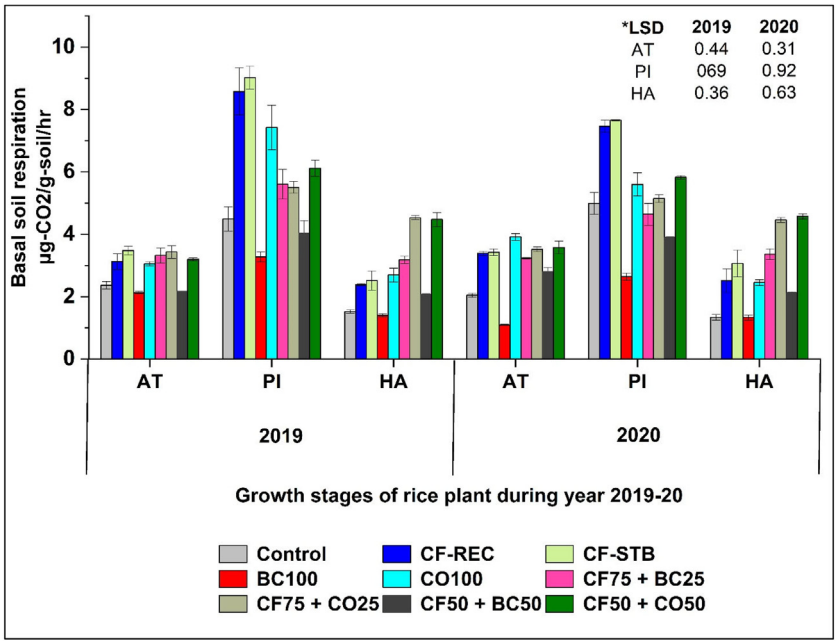

Fig. 7. Basal soil respiration. The basal soil respiration as affected by different nutrient management treatments in paddy soil in year 2019–2020 at Active tillering (AT), Panicle initiation (PI) and Harvest (HA) growth stages of rice plant grown in controlled environment experiment. *LSD represents Fisher's Least Significant Difference ($p = 0.05$) among the treatments indicated by different colour bars.

farming on electricity (e.g., for irrigation), which results in more demand for power from thermal power plants (Source: Census and Economic Information Center data). In India, the total cropped area has increased between 2005 and 2015 leading to an increase in the total farm power availability from 1.50 kW/ha in 2005 to 1.94 kW/ha in 2012 (Figure S4). The share of electric motor is also increasing, due to which the electricity consumption in agriculture has grown at 5.63% (CAGR) from 2009 to 2018 (Source: State of Indian Agriculture 2017–18). As per EDGAR data the electricity and heat production emitting around 54% more CO_2 into the atmosphere in 2018 as compared to 2009.

The total energy consumption in India has also increased by about 50% during the last decade, making it the fifth largest energy consumer globally by using about 4.4% of the world's total energy (Source: US Energy Information Administration data). Apart from these, India is the second largest cement producer in the world and accounted for over 8% of the global installed capacity as of 2019. This also suggests the demand for building farm infrastructures and storage facilities for maintaining the cold chain to market. The cement production in India has increased from 186 MMT in FY (Financial Year) 2009 to 337 MMT in FY 2019 (Source: Indiastat.com). There is around 36% increase in CO_2 emissions from cement production in India between 2009 and 2018. Therefore, all these factors are responsible for the increasing trends of CO_2 concentration in India during the past decades.

3.4. Soil respiration and paddy crop yield as affected by different nutrient management strategies

The terrestrial exchange of carbon plays a vital role in regulating the global carbon cycle in the biosphere (Barichivich et al., 2013; Forkel et al., 2016; Graven et al., 2013). The CO_2 concentration in the atmosphere is strongly influenced by soil respiration and vegetation cover. Soil respiration acts as a key process in the total carbon flow to the atmosphere thus, influencing global carbon cycle and is primarily regulated by microbial activity (Schlesinger and Andrews, 2000). Therefore, modification of soil respiration may alter atmospheric CO_2 concentration at a global scale (Schlesinger and Andrews, 2000). Furthermore, soil respiration (which is the CO_2 produced by the biological activity of soil organisms), is the major flux within the global carbon cycle, emitting about ten times more CO_2 to the atmosphere annually than fossil fuel combustion (Bond-Lamberty and Thomson, 2010).

Basal soil respiration indicates microbial mineralization of soil organic matter (SOM) stock leading to output of CO_2 from soil, which is strongly related to the types and amount of carbon input to soil (Zhang et al., 2019). Stable carbon inputs like sole biochar application (BC100) reduced the soil respiration in both the years (Table 1). However, the reduction in soil respiration was comparatively higher in 2020 than that in 2019 (Fig. 7). However, the integrated application of biochar with chemical fertilizers (CF75+BC25 and CF50+BC 50) did not change significantly in both years. The highest soil respiration in all the nutrient management treatments was observed during the panicle initiation stage of paddy in both years, which can be attributed to the role of root exudates promoting microbial oxidation of soil carbon (Canarini

et al., 2019; Zhang et al., 2019). However, resistant carbon alternatives like compost application (CO100) lead to increased soil respiration during panicle initiation in 2020 compared to that in 2019, which might be due to the residual effect of compost application in paddy crops. The highest (7.4–8.6 μg-CO2/g-soil/hr) carbon emission is observed with chemical fertilizer application to paddy soil, as they serve as a readily available source of nitrogen in microbial metabolism. However, chemical fertilizers when applied in an integrated manner (INM) with compost (CF75+CO25 and CF50+CO50) or biochar (CF75+BC25 and CF50+BC50) reduced the soil respiration than the sole application of compost or chemical fertilizer, but it emitted more CO_2 than that by sole biochar application (BC100).

Our results agree with Wei et al. (2021), who reported decreased soil respiration with biochar application. We observe that increasing doses of biochar (e.g., CF75+BC25, CF50+BC50 and BC100) reduce the soil respiration progressively and is evident in all three growth stages of rice in both years. The reduction in microbe-mediated soil respiration can be attributed to the immobilization of organic acids and messenger molecules required in bacterial quorum sensing with increasing doses of biochar (Gao et al., 2016; Zhong et al., 2020). However, the results for soil respiration in the case of compost application were just the opposite of biochar, which showed the highest emission (5.5–8.09 μg-CO_2/g-soil/hr) with maximum dose (CO100). Therefore, results of our analyses indicate that biochar can be a better substitute of compost in the nutrient management strategies of paddy with lower soil respiration. However, our results for grain yield per hill of paddy were highest (37.65 g $hill^{-1}$) in low dose biochar-based INM treatment (Table 1); indicating better nutrient uptake in the low dose biochar treatment. Henceforth, findings indicate that biochar fertilizer in low doses can be a beneficial strategy in the sustainable yield improvement of paddy. The improved yield indirectly lowers the burden on environment through reduced yield scaled CO_2 emissions (i.e., CO_2 per kg grain produced), while addition of biochar as a stable carbon source to soil acts as a direct abatement to atmospheric CO_2. The fixed atmospheric CO_2 as biochar in stable heterocyclic aromatic forms remains in soil for millennia (Abbhishek et al., 2021). Our findings with this pilot scale study further indicates that the addition of biochar as a nutrient carrier to the prominent rice based cropping systems thus can have significant effect on net removal of CO_2 from ecosystem.

4. Conclusion

Atmospheric CO_2 shows significant changes in different agricultural seasons in India. *Zaid* season shows the highest concentration, whereas the lowest concentration in the *kharif* season. Atmospheric CO_2 concentrations over India are mainly controlled by vegetation, which acts as a strong sink for atmospheric CO_2 through photosynthesis. The highest CO_2 concentration is observed during the *zaid* season owing to the lack of vegetation and strong convection. In addition, the dry season combined with high daytime temperature during April–May create a tendency for the ecosystem to become a moderate source of carbon exchange. The lowest CO_2 concentration observed in the *kharif* season is because of the heavy rainfall and high vegetation cover during these months. However, in the *rabi* season the CO_2 concentration rises gradually as the soil moisture recedes slowly, and plants are also in slow growing stage. As a result, respiration takes over the weak photosynthesis, contributing to increasing levels of CO_2 concentration in the atmosphere. Our agro-management analyses indicate that the management non-intensive period (January to June) is the least productive period in terms of NPP in India. As a result, higher CO_2 concentration is observed during this period. The atmospheric CO_2 showed an increasing trend of 2.42 ppm/year over India in 2009–2020. Anthropogenic activities such as biomass burning, coal, fossil fuels and energy consumption also contribute significantly to this increasing trend of CO_2 emissions. Our trajectory analysis show that the long-range transport along with local sources are also responsible for the high CO_2 in India. We also find that the edaphic CO_2 emissions mediated by soil microbes can be significantly reduced by using stable carbon like biochar in place of resistant carbon (e.g., compost) in nutrient management practices of paddy. Our analyses can give a means to better comprehend the spatiotemporal changes in CO_2 concentration over India originating from the agricultural activities such as biomass burning and agricultural management. Furthermore, our study highlights the important drivers of increasing trends in atmospheric CO_2 over India, e.g., vegetation and human activities. This could also have an enlightening influence on policy interventions aimed to curb the increase of CO_2 concentration over India. However, this study determined the relative contributions of the primary determining variables of CO_2 qualitatively, without quantifying the specific contributions of each factor. Therefore, a later study would focus on quantitatively attributing the effects of these components, including air transport as well as atmospheric dynamics at various scales.

CRediT authorship contribution statement

A. Singh: First draft was made, Discussion and a subsequent final draft was made, Data analysis, The figures were made. **K. Abbhishek:** First draft was made, Discussion and a subsequent final draft was made, The pot-experiments and analyses are conducted, The figures were made. **J. Kuttippurath:** Conceptualization, Methodology, Designed, First draft was made, Discussion and a subsequent final draft was made, The figures were made, Supervision, Project management. **S. Raj:** Discussion and a subsequent final draft was made, The figures were made. **N. Mallick:** Discussion and a subsequent final draft was made, Supervision, Project management. **G. Chander:** Discussion and a subsequent final draft was made, Supervision. **S. Dixit:** Discussion and a subsequent final draft was made, Supervision.

Declaration of competing interest

The authors declare that they have no known competing financial interests or personal relationships that could have appeared to influence the work reported in this paper.

Data availability

The data used in this study are publicly available. The GOSAT satellite data are available on https://data2.gosat.nies.go.jp/GosatDataArchiveService/usr/download/DownloadPage/view. The GFED data are taken from https://www.globalfiredata.org/index.html. The Net stock change (C) over cropland organic soils, agriculture land use (ALU) CO_2 emissions and mineral fertilizer data are taken from http://www.fao.org/faostat/en/#data. The ODIAC CO_2 emissions data are taken from https://odiac.org/index.html. Agriculture cropped area and share of total power data are available at http://www.indiastatagri.com/. Total energy consumption data of India is available at https://www.eia.gov/international/data/country/IND. Census and Economic Information Center data is available at https://www.ceicdata.com/en/indicator/india/coal-consumption. State of Indian Agriculture 2017–18 report is available at https://eands.dacnet.nic.in/PDF/State_of_Indian_Agriculture,2017.pdf. Cement production data of India is taken from https://www.indiastat.com/Home/DataSearch. Indian petroleum & natural gas statistics 2019-20 report is available at https://mopng.gov.in/files/TableManagements/IPNG-2019-20.pdf. The NEE data are available at https://www.nies.go.jp/doi/10.17595/20200227.001-e.html#block2. The NPP data are taken from https://neo.gsfc.nasa.gov/view.php?datasetId=MOD17A2_M_PSN. The NDVI data are available at https://neo.gsfc.nasa.gov/view.php?datasetId=MOD_NDVI_M.

Acknowledgements

We thank the Chairman, CORAL and Agricultural and Food Engineering (AgFE), and the Director, Indian Institute of Technology Kharagpur, Ministry of Education (MoE). AS and KA thank MOE and IIT KGP for the PhD fellowship. SR acknowledges the support through the NRB and DRDO project. We also thank all the data managers and the scientists who made available those data for this study. We thank IMD (India Meteorological Department/MoES) for precipitation and temperature data. The MODIS datasets were acquired from the Level-3 and Atmosphere Archive and Distribution System (LAADS) Distributed Active Archive Center (DAAC), located in the Goddard Space Flight Center in Greenbelt, Maryland (https://ladsweb.nascom.nasa.gov/). We also acknowledge Directorate of Economics and Statistics, Department of Agriculture and Cooperation, India; Department of Animal Husbandry, Dairying & Fisheries, India; Ministry of Petroleum and Natural Gas, India for the agricultural, livestock and gas and oil statistical data. We would like to thank the entire GOSAT team for their dedicated and continuous efforts in producing the data for all these years. We acknowledge the assistance provided by the International Crops Research Institute for Semiarid Tropics (ICRISAT) and ICRISAT Development Center (IDC) for providing all required experimental facilities.

Appendix A. Supplementary data

Supplementary material related to this article can be found online at https://doi.org/10.1016/j.eti.2022.102498.

References

Abbhishek, K., Chander, G., Dixit, S., Kuttippurath, J., et al., 2021. Legume biochar fertilizer can be an efficient alternative to compost in integrated nutrient management of paddy (*Oryza sativa l.*). J. Soil Sci. Plant Nutr. 21, 2673–2688. http://dx.doi.org/10.1007/s42729-021-00555-4.

Anthwal, A., Joshi, V., Joshi, S., Sharma, A., Kim, K.-H., 2009. Atmospheric carbon dioxide levels in Garhwal Himalaya. India. J. Korean Earth Sci. Soc. 30, 588–597. http://dx.doi.org/10.5467/jkess.2009.30.5.588.

Barichivich, J., Briffa, K.R., Myneni, R.B., Osborn, T.J., Melvin, T.M., Ciais, P., Piao, S., Tucker, C., 2013. Large-scale variations in the vegetation growing season and annual cycle of atmospheric CO_2 at high northern latitudes from 1950 to 2011. Glob. Chang. Biol. 19, 3167–3183. http://dx.doi.org/10.1111/gcb.12283.

Behringer, D., Xue, Y., 2004. Evaluation of the global ocean data assimilation system at NCEP:the pacific ocean. In: Eighth Symposium on Integrated Observing and Assimilation Systems for Atmosphere, Oceans, and Land Surface. Seattle, Washington, vol. 1. pp. 1–15.

Bhuyan, R., 2019. Review note on shifting cultivation in northeast India amidst changing perceptions. Dhaulagiri J. Sociol. Anthropol. 13, 90–95. http://dx.doi.org/10.3126/dsaj.v13i0.24252.

Boesch, H., Baker, D., Connor, B., Crisp, D., Miller, C., 2011. Global characterization of CO_2 column retrievals from shortwave-infrared satellite observations of the orbiting carbon observatory-2 mission. Remote Sens. 3, 270–304. http://dx.doi.org/10.3390/rs3020270.

Bond-Lamberty, B., Thomson, A., 2010. Temperature-associated increases in the global soil respiration record. Nature 464, 579–582. http://dx.doi.org/10.1038/nature08930.

Brenzinger, K., Drost, S.M., Korthals, G., Bodelier, P.L.E., 2018. Organic residue amendments to modulate greenhouse gas emissions from agricultural soils. Front. Microbiol. 9 (3035), http://dx.doi.org/10.3389/fmicb.2018.03035.

Buchwitz, M., Reuter, M., Schneising, O., Noël, S., Gier, B., Bovensmann, H., Burrows, J.P., Boesch, H., Anand, J., Parker, R.J., Somkuti, P., Detmers, R.G., Hasekamp, O.P., Aben, I., Butz, A., Kuze, A., Suto, H., Yoshida, Y., Crisp, D., O'Dell, C., 2018. Computation and analysis of atmospheric carbon dioxide annual mean growth rates from satellite observations during 2003–2016. Atmos. Chem. Phys. 18, 17355–17370. http://dx.doi.org/10.5194/acp-18-17355-2018.

Canarini, A., Kaiser, C., Merchant, A., Richter, A., Wanek, W., 2019. Root exudation of primary metabolites: Mechanisms and their roles in plant responses to environmental stimuli. Front. Plant Sci. 10, http://dx.doi.org/10.3389/fpls.2019.00157.

Case, S.D.C., McNamara, N.P., Reay, D.S., Whitaker, J., 2014. Can biochar reduce soil greenhouse gas emissions from a miscanthus bioenergy crop? GCB Bioenergy 6, 76–89. http://dx.doi.org/10.1111/gcbb.12052.
Chai, R., Ye, X., Ma, C., Wang, Q., Tu, R., Zhang, L., Gao, H., 2019. Greenhouse gas emissions from synthetic nitrogen manufacture and fertilization for main upland crops in China. Carbon Balance Manag. 14, 1–10. http://dx.doi.org/10.1186/s13021-019-0133-9.
Chhabra, A., Gohel, A., 2019. Dynamics of atmospheric carbon dioxide over different land cover types in India. Environ. Monit. Assess. 191, http://dx.doi.org/10.1007/s10661-019-7681-z.
Clark, D.A., Brown, S., Kicklighter, D.W., Chambers, J.Q., Thomlinson, J.R., Ni, J., Holland, E.A., 2001. Net primary production in tropical forests: An evaluation and synthesis of existing field data. Ecol. Appl. 11, 371–384. http://dx.doi.org/10.1890/1051-0761(2001)011[0371:NPPITF]2.0.CO;2.
Daniel, Taub R., 2010. Effects of rising atmospheric concentrations of carbon dioxide on plants | learn science at scitable [www document]. Nat. Educ. Knowl. 3 (10), 21, URL https://www.nature.com/scitable/knowledge/library/effects-of-rising-atmospheric-concentrations-of-carbon-13254108/. (Accessed 26 May 2021).
Dlugokencky, E., Tans, P., 2015. Trends in atmospheric carbon dioxide. http://www.esrl.noaa.gov/gmd/ccgg/trends.
Dubash, N.K., Khosla, R., Rao, N.D., Bhardwaj, A., 2018. India's energy and emissions future: An interpretive analysis of model scenarios. Environ. Res. Lett. 13 (7), http://dx.doi.org/10.1088/1748-9326/aacc74.
Ekwurzel, B., Boneham, J., Dalton, M.W., Heede, R., Mera, R.J., Allen, M.R., Frumhoff, P.C., 2017. The rise in global atmospheric CO_2, surface temperature, and sea level from emissions traced to major carbon producers. Clim. Change 144 (4), 579–590. http://dx.doi.org/10.1007/s10584-017-1978-0.
Food and Agriculture Organization of the United Nations (FAO), 2019. Faostat statistical database, statistical division. Rome.
Forkel, M., Carvalhais, N., Rödenbeck, C., Keeling, R., Heimann, M., Thonicke, K., Zaehle, S., Reichstein, M., 2016. Enhanced seasonal CO_2 exchange caused by amplified plant productivity in northern ecosystems. Science 351 (80-.), 696–699. http://dx.doi.org/10.1126/science.aac4971.
Gao, X., Cheng, H.Y., Valle, I.Del., Liu, S., Masiello, C.A., Silberg, J.J., 2016. Charcoal disrupts soil microbial communication through a combination of signal sorption and hydrolysis. ACS Omega 1, 226–233. http://dx.doi.org/10.1021/acsomega.6b00085.
Graven, H.D., Keeling, R.F., Piper, S.C., Patra, P.K., Stephens, B.B., Wofsy, S.C., Welp, L.R., Sweeney, C., Tans, P.P., Kelley, J.J., Daube, B.C., Kort, E.A., Santoni, G.W., Bent, J.D., 2013. Enhanced seasonal exchange of CO2 by northern ecosystems since 1960. Science 341 (80-.), 1085–1089.
Gupta, A., Dhaka, S.K., Matsumi, Y., Imasu, R., Hayashida, S., Singh, V., 2019. Seasonal and annual variation of AIRS retrieved CO 2 over India during 2003–2011. J. Earth Syst. Sci. 128, 1–12. http://dx.doi.org/10.1007/s12040-019-1108-7.
Gurney, K.R., Law, R.M., Denning, A.S., Rayner, P.J., Baker, D., Bousquet, P., Bruhwiler, L., Chen, Y.H., Ciais, P., Fan, S., Fung, I.Y., Gloor, M., Heimann, M., Higuchi, K., John, J., Maki, T., Maksyutov, S., Masarie, K., Peylin, P., Prather, M., Pak, B.C., Randerson, J., Sarmiento, J., Taguchi, S., Takahashi, T., Yuen, C.W., 2002. Towards robust regional estimates of annual mean {co}_2 sources and sinks. Nature 415, 626–630.
Haney, R.L., Brinton, W.F., Evans, E., 2002. Soil CO 2 respiration: Comparison of chemical titration. In: CO 2 IRGA Analysis and the Solvita Gel System. http://dx.doi.org/10.1017/S174217050800224X.
Heinze, C., Meyer, S., Goris, N., Anderson, L., Steinfeldt, R., Chang, N., Quéré, C.Le., Bakker, D.C.E., 2015. The ocean carbon sink - impacts, vulnerabilities and challenges. Earth Syst. Dyn. 6, 327–358.
Iavorivska, L., Boyer, E.W., DeWalle, D.R., 2016. Atmospheric deposition of organic carbon via precipitation. Atmos. Environ. 146, 153–163. http://dx.doi.org/10.1016/j.atmosenv.2016.06.006.
Inoue, M., Morino, I., Uchino, O., Miyamoto, Y., Yoshida, Y., Yokota, T., Machida, T., Sawa, Y., Matsueda, H., Sweeney, C., Tans, P.P., Andrews, A.E., Biraud, S.C., Tanaka, T., Kawakami, S., Patra, P.K., 2013. Validation of XCO2 derived from SWIR spectra of GOSAT TANSO-FTS with aircraft measurement data. Atmos. Chem. Phys. 13, 9771–9788. http://dx.doi.org/10.5194/acp-13-9771-2013.
IPCC, 2018. Special Report on Global Warming of 1.5°C (Report). Incheon, Republic of Korea: Intergovernmental Panel on Climate Change (IPCC), Retrieved 7 October 2018.
Jin, Q., Wei, J., Lau, W.K.M., Pu, B., Wang, C., 2021. Interactions of Asian mineral dust with Indian summer monsoon: Recent advances and challenges. Earth-Sci. Rev. 215, 103562. http://dx.doi.org/10.1016/j.earscirev.2021.103562.
Kaur, J., Singh, A., 2017. Direct seeded rice: Prospects, problems/constraints and researchable issues in India. Curr. Agric. Res. J. 5, 13–32. http://dx.doi.org/10.12944/carj.5.1.03.
Kramer, K., Leinonen, I., Bartelink, H.H., et al., 2002. Evaluation of six process-based forest growth models using eddy-covariance measurements of CO_2 and H_2o fluxes at six forest sites in Europe. Glob. Change Biol. 8, 213–230, https://onlinelibrary.wiley.com/doi/abs/10.1046/j.1365-2486.2002.00471.x.
Krishnapriya, M., Nayak, R.K., Allahudeen, S., Bhuvanachandra, A., Dadhwal, V.K., Jha, C.S., Sheshasai, M.V.R., Sasmal, S.K., Prasad, K.V.S.R., 2020. Seasonal variability of tropospheric CO_2 over India based on model simulation, satellite retrieval and in-situ observation. J. Earth Syst. Sci. 129, http://dx.doi.org/10.1007/s12040-020-01478-x.
Kuttippurath, J., Murasingh, S., Stott, P.A., Sarojini, B.Balan., Jha, M.K., Kumar, P., Nair, P.J., Varikoden, H., Raj, S., Francis, P.A., Pandey, P.C., 2021. Observed rainfall changes in the past century over the wettest place on Earth (1901–2019). Environ. Res. Lett. 16, http://dx.doi.org/10.1088/1748-9326/abcf78.
Kuttippurath, J., Raj, S., 2021. Two decades of aerosol observations by AATSR, MISR, MODIS and MERRA-2 over India and Indian ocean. Remote Sens. Environ. 257, 112363. http://dx.doi.org/10.1016/j.rse.2021.112363.
Kuttippurath, J., Singh, A., Dash, S.P., Mallick, N., Clerbaux, C., Damme, M.Van., Clarisse, L., Coheur, P.F., Raj, S., Abbhishek, K., Varikoden, H., 2020. Record high levels of atmospheric ammonia over India: Spatial and temporal analyses. Sci. Total Environ. 740, http://dx.doi.org/10.1016/j.scitotenv.2020.139986.
Kuze, A., Suto, H., Nakajima, M., Hamazaki, T., 2009. Thermal and near infrared sensor for carbon observation Fourier-transform spectrometer on the greenhouse gases observing satellite for greenhouse gases monitoring. Appl. Opt. 48, 6716–6733. http://dx.doi.org/10.1364/AO.48.006716.
Lakshmanan, P.K., Singh, S., Lakshmi, S.Asta., 2017. The Paris agreement on climate change and India. J. Clim. Chang. 3, 1–10. http://dx.doi.org/10.3233/jcc-170001.
Lal, R., 2019. Accelerated soil erosion as a source of atmospheric CO 2. Soil Tillage Res. 188, 35–40. http://dx.doi.org/10.1016/j.still.2018.02.001.
Lal, R., Pimentel, D., 2008. Soil erosion: A carbon sink or source? Science 319 (5866), 1040–1042. http://dx.doi.org/10.1126/%20science.319.5866.1040.
Le Quere, C., Raupach, M.R., Canadell, J.G., Marland, G., Bopp, L., Ciais, P., Conway, T.J., Doney, S.C., Feely, R.A., Foster, P., Friedlingstein, P., Gurney, K., Houghton, R.A., House, J.I., Huntingford, C., Levy, P.E., Lomas, M.R., Majkut, J., Metzl, N., Ometto, J.P., Peters, G.P., Prentice, I.C., Randerson, J.T., Running, S.W., Sarmiento, J.L., Schuster, U., Sitch, S., Takahashi, T., Viovy, N., Van Der Werf, G.R., Woodward, F.I., 2009. Trends in the sources and sinks of carbon dioxide. Nat. Geosci. 2, 831–836. http://dx.doi.org/10.1038/ngeo689.
Leung, D.Y.C., Caramanna, G., Maroto-Valer, M.M., 2014. An overview of current status of carbon dioxide capture and storage technologies. Renew. Sustain. Energy Rev. 39, 426–443. http://dx.doi.org/10.1016/j.rser.2014.07.09.
Mahesh, P., Sreenivas, G., Rao, P.V.N., Dadhwal, V.K., 2016. Atmospheric CO₂retrieval from ground based FTIR spectrometer over shadnagar. India. Atmos. Meas. Tech. Discuss 1–10. http://dx.doi.org/10.5194/amt-2016-177.
Morino, I., Uchino, O., Inoue, M., Yoshida, Y., Yokota, T., Wennberg, P.O., Toon, G.C., Wunch, D., Roehl, C.M., Notholt, J., Warneke, T., Messerschmidt, J., Griffith, D.W.T., Deutscher, N.M., Sherlock, V., Connor, B., Robinson, J., Sussmann, R., Rettinger, M., 2011. Preliminary validation of column-averaged volume mixing ratios of carbon dioxide and methane retrieved from GOSAT short-wavelength infrared spectra. Atmos. Meas. Tech. 4, 1061–1076. http://dx.doi.org/10.5194/amt-4-1061-2011.

Morino, I., Uchino, Y., Tsutsumi, H., Ohyama, T.T.N., Trieu, Y., Yoshida, T., Matsunaga, A., Kamei, M., Saito, H., Noda, I., Morino, O., Uchino, Y., Tsutsumi, H., Ohyama, T.T.N., Trieu, Y., Yoshida, T., Matsunaga, A., Kamei, M., Saito, H., Noda, O., 2019. Progress on GOSAT and GOSAT–2 FTS SWIR L2 validation AGUFM, (2019). A41S-2640.

Nalini, K., Uma, K.N., Sijikumar, S., Tiwari, Y.K., Ramachandran, R., 2018. Satellite- and ground-based measurements of CO_2 over the Indian region: its seasonal dependencies, spatial variability, and model estimates. Int. J. Remote Sens. 39, 7881–7900. http://dx.doi.org/10.1080/01431161.2018.1479787.

Nayak, R.K., Dadhwal, V.K., Majumdar, A., Patel, N.R., Dutt, C.B.S., 2011. Variability of atmospheric co₂over india and surrounding oceans and control by surface fluxes. ISPRS - Int. Arch. Photogramm. Remote Sens. Spat. Inf. Sci. XXXVIII-8/9, 6–101. http://dx.doi.org/10.5194/isprsarchives-xxxviii-8-w20-96-2011.

Nayak, M., Swain, D.K., Sen, R., 2019. Strategic valorization of de-oiled microalgal biomass waste as biofertilizer for sustainable and improved agriculture of rice (*Oryza sativa l.*)crop. Sci. Total Environ. 682, 475–484. http://dx.doi.org/10.1016/j.scitotenv.2019.05.123.

Neue, H., 1993. Methane emission from rice fields: Wetland rice fields may make a major contribution to global warming. Biosci 43, 466–472.

Oda, T., Maksyutov, S., 2011. A very high-resolution (1km $\times$1 km) global fossil fuel CO_2 emission inventory derived using a point source database and satellite observations of nighttime lights. Atmos. Chem. Phys. 11, 543–556. http://dx.doi.org/10.5194/acp-11-543-2011.

Olivier, J.G.J., Peters, J.A.H.W., 2019. Trends in Global CO_2 and Total Greenhouse Gas Emissions. 2019 Report, PBL Netherlands Environmental Assessment Agency, The Hague.

Pasha, S.V., Behera, M.D., Mahawar, S.K., Barik, S.K., Joshi, S.R., 2020. Assessment of shifting cultivation fallows in northeastern India using landsat imageries. Trop. Ecol. 61, 65–75. http://dx.doi.org/10.1007/s42965-020-00062-0.

Patra, P.K., Canadell, J.G., Houghton, R.A., Piao, S.L., Oh, N.H., Ciais, P., Manjunath, K.R., Chhabra, A., Wang, T., Bhattacharya, T., Bousquet, P., Hartman, J., Ito, A., Mayorga, E., Niwa, Y., Raymond, P.A., S. Sarma, V.V.S., Lasco, R., 2013. The carbon budget of South Asia. Biogeosciences 10, 513–527. http://dx.doi.org/10.5194/bg-10-513-2013.

Prasad, P., Rastogi, S., Singh, R.P., 2014. Study of satellite retrieved CO 2 and CH 4 concentration over India. Adv. Sp. Res. 54, 1933–1940. http://dx.doi.org/10.1016/j.asr.2014.07.021.

Preethi, B., Revadekar, J.V., Kripalani, R.H., 2011. Anomalous behaviour of the Indian summer monsoon 2009. J. Earth Syst. Sci. 120, 783–794. http://dx.doi.org/10.1007/s12040-011-0112-3.

Schinner, F., Ohlinger, R., Kandeler, M.F. (Eds.), 1995. Methods in Soil Biology. Springer US, M. in S.B.S.U..

Schlesinger, W.H., Andrews, J.A., 2000. Soil respiration and the global carbon cycle. Biogeochemistry 48, 7–20. http://dx.doi.org/10.1023/A:1006247623877.

Sharma, N., Dadhwal, V.K., Kant, Y., Mahesh, P., Mallikarjun, K., Gadavi, H., Sharma, A., Ali, M.M., 2014. Atmospheric CO_2 variations in two contrasting environmental sites over India. Air, Soil Water Res. 7, 61–68. http://dx.doi.org/10.4137/ASWR.S13987.

Sharma, N., Nayak, R.K., Dadhwal, V.K., Kant, Y., Ali, M.M., 2012. Temporal variations of atmospheric CO_2 in dehradun, India during 2009. Air, Soil Water Res 6, 37–45. http://dx.doi.org/10.4137/ASWR.S10590.

Shi, Y., Matsunaga, T., Noda, H., 2017. Interpreting temporal changes of atmospheric CO_2 over fire affected regions based on GOSAT observations. IEEE Geosci. Remote Sens. Lett. 14, 77–81. http://dx.doi.org/10.1109/LGRS.2016.2627056.

Shusterman, A., Kim, J., Lieschke, K., Newman, C., Wooldridge, P., Cohen, R., 2018. Observing local CO2 sources using low-cost, near-surface urban monitors. Atmos. Chem. Phys. 18 (18), 13773–13785. http://dx.doi.org/10.5194/acp-18-13773-2018.

Singh, A., Kuttippurath, J., Abbhishek, K., Mallick, N., Raj, S., Chander, G., Dixit, S., 2021. Biogenic link to the recent increase in atmospheric methane over India. http://dx.doi.org/10.1016/j.jenvman.2021.112526.

Sirois, A., Bottenheim, J.W., 1995. Use of backward trajectories to interpret the 5-year record of PAN and OSUB 3 ambient air concentrations at Kejimkujik National Park. Nova Scotia. J. Geophys. Res. 100, 2867–2881. http://dx.doi.org/10.1029/94JD02951.

Smith, P., Martino, D., Cai, Z., Gwary, D., Janzen, H., Kumar, P., McCarl, B., Ogle, S., O'Mara, F., Rice, C., Scholes, B., Sirotenko, O., Howden, M., McAllister, T., Pan, G., Romanenkov, V., Schneider, U., Towprayoon, S., 2007. Policy and technological constraints to implementation of greenhouse gas mitigation options in agriculture. Agric. Ecosyst. Environ. 118, 6–28. http://dx.doi.org/10.1016/j.agee.2006.06.006.

Sreenivas, G., Mahesh, P., Subin, J., Kanchana, A.L., Venkata, P., Rao, N., Dadhwal, V.K., 2016. Influence of meteorology and interrelationship with greenhouse gases (CO 2 and CH 4) at a suburban site of India. Atmos. Chem. Phys. 16, 3953–3967. http://dx.doi.org/10.5194/acp-16-3953-2016.

Stein, A.F., Draxler, R.R., Rolph, G.D., Stunder, B.J.B., Cohen, M.D., Ngan, F., 2015. Noaa's hysplit atmospheric transport and dispersion modeling system. Bull. Am. Meteorol. Soc. 96, 2059–2077. http://dx.doi.org/10.1175/BAMS-D-14-00110.1.

Tiwari, Y.K., Patra, P.K., Chevallier, F., Francey, R.J., Krummel, P.B., Allison, C.E., Revadekar, J.V., Chakraborty, S., Langenfelds, R.L., Bhattacharya, S.K., Borole, D.V., Kumar, K.R., Steele, L.P., 2011. Carbon dioxide observations at Cape Rama, India for the period 1993-2002: implications for constraining Indian emissions. Curr. Sci. 101, 1562–1568.

Tiwari, Y.K., Revadekar, J.V., Kumar, K.Ravi., 2013. Variations in atmospheric carbon dioxide and its association with rainfall and vegetation over India. Atmos. Environ. 68, 45–51. http://dx.doi.org/10.1016/j.atmosenv.2012.11.040.

Van Der Werf, G.R., Randerson, J.T., Giglio, L., Van Leeuwen, T.T., Chen, Y., Rogers, B.M., Mu, M., Van Marle, M.J.E., Morton, D.C., Collatz, G.J., Yokelson, R.J., Kasibhatla, P.S., 2017. Global fire emissions estimates during 1997–2016. Earth Syst. Sci. Data 9, 697–720. http://dx.doi.org/10.5194/essd-9-697-2017.

Venkataraman, C., Habib, G., Kadamba, D., Shrivastava, M., Leon, J.F., Crouzille, B., Boucher, O., Streets, D.G., 2006. Emissions from open biomass burning in India: Integrating the inventory approach with high-resolution moderate resolution imaging spectroradiometer (MODIS) active-fire and land cover data. Glob. Biogeochem. Cycles 20, 1–12. http://dx.doi.org/10.1029/2005GB002547.

Watanabe, H., Hayashi, K., Saeki, T., Maksyutov, S., Nasuno, I., Shimono, Y., Hirose, Y., Takaichi, K., Kanekon, S., Ajiro, M., Matsumoto, Y., Yokota, T., 2015. Global mapping of greenhouse gases retrieved from GOSAT level 2 products by using a kriging method. Int. J. Remote Sens. 36, 1509–1528. http://dx.doi.org/10.1080/01431161.2015.1011792.

Wei, Z., Wang, J.J., Fultz, L.M., White, P., Jeong, C., 2021. Application of biochar in estrogen hormone-contaminated and manure-affected soils: Impact on soil respiration, microbial community and enzyme activity. Chemosphere 270, 128625. http://dx.doi.org/10.1016/j.chemosphere.2020.128625.

Yang, Y., Zhao, Y., 2018. Quantification and evaluation of atmospheric pollutant emissions from open biomass burning with multiple methods: A case study for Yangtze River Delta region. China. Atmos. Chem. Phys. 1–44. http://dx.doi.org/10.5194/acp-2018-701.

Zeng, J., Matsunaga, T., Tan, Z.H., et al., 2020. Global terrestrial carbon fluxes of 1999–2019 estimated by upscaling eddy covariance data with a random forest. Sci. Data 7 (313).

Zhang, S., Hussain, H.A., Wang, L., Hussain, S., Li, B., Zhou, H., Luo, H., Zhang, X., Ma, Z., Long, L., Dai, Y., 2019. Responses of soil respiration and organic carbon to straw mulching and ridge tillage in maize field of a triple cropping system in the hilly region of southwest China. Sustain. 11, http://dx.doi.org/10.3390/su11113068.

Zhang, M., Zhang, X.Y., Liu, R.X., Hu, L.Q., 2014. A study of the validation of atmospheric CO_2 from satellite hyper spectral remote sensing. Adv. Clim. Chang. Res. 5, 131–135. http://dx.doi.org/10.1016/j.accre.2014.11.002.

Zhong, Y., Igalavithana, A.D., Zhang, M., Li, X., Rinklebe, J., Hou, D., Tack, F.M.G., Alessi, D.S., Tsang, D.C.W., Ok, Y.S., 2020. Effects of aging and weathering on immobilization of trace metals/metalloids in soils amended with biochar. Environ. Sci. Process. Impacts 22, 1790–1808. http://dx.doi.org/10.1039/d0em00057d.